

1
2
3
4
5
6
7
8
9
10
11
12
13
14
15
16
17
18
19
20
21
22
23
24
25
26
27
28
29
30
31
32
33
34
35
36
37
38
39
40
41
42
43
44
45

**Selective nuclear export of mRNAs is promoted by DRBD18 in
*Trypanosoma brucei***

Amartya Mishra^{1*}, Jan Naseer Kaur^{1*}, Daniel I. McSkimming², Eva Hegedúsová³, Ashutosh P. Dubey¹, Martin Ciganda¹, Zdeněk Paris^{3,4}, and Laurie K. Read¹

¹University at Buffalo, Jacobs School of Medicine and Biomedical Sciences, Buffalo, NY, USA; ²Bioinformatics and Computational Biology Core, University of Southern Florida, Tampa, FL, USA; ³Institute of Parasitology, Biology Centre, Czech Academy of Sciences, České Budějovice (Budweis), Czech Republic, ⁴Faculty of Science, University of South Bohemia České Budějovice (Budweis), Czech Republic.

Running title: DRBD18 controls mRNA export in *Trypanosoma brucei*

Keywords: Trypanosome, RNA binding protein, mRNA export, RNAseq, FISH, Nucleoporin

*equal contribution

To whom correspondence should be addressed:

Laurie K. Read

lread@buffalo.edu

716-829-3307

1 **SUMMARY**

2 Kinetoplastids, including *Trypanosoma brucei*, control gene expression primarily at the
3 posttranscriptional level. Nuclear mRNA export is an important, but understudied, step in this
4 process. The general heterodimeric export factors, Mex67/Mtr2, function in the export of mRNAs
5 and tRNAs in *T. brucei*, but RNA binding proteins (RBPs) that regulate export processes by
6 controlling the dynamics of Mex67/Mtr2 ribonucleoprotein formation or transport have not been
7 identified. Here, we report that DRBD18, an essential and abundant *T. brucei* RBP, associates with
8 Mex67/Mtr2 *in vivo*, likely through its direct interaction with Mtr2. DRBD18 downregulation
9 results in partial accumulation of poly(A)⁺ mRNA in the nucleus, but has no effect on localization
10 of intron-containing or mature tRNAs. Comprehensive analysis of transcriptomes from whole cell
11 and cytosol in DRBD18 knockdown parasites demonstrates that depletion of DRBD18 leads to
12 impairment of nuclear export of a subset of mRNAs. CLIP experiments reveal association of
13 DRBD18 with several of these mRNAs. Moreover, DRBD18 knockdown leads to a partial
14 accumulation of the Mex67/Mtr2 export receptors in the nucleus. Taken together, the current study
15 supports a model in which DRBD18 regulates the selective nuclear export of mRNAs by
16 promoting the mobilization of export competent mRNPs to the cytosol through the nuclear pore
17 complex.

1 **1 INTRODUCTION**

2 *Trypanosoma brucei* species are early diverged unicellular eukaryotic parasites causing African
3 Sleeping Sickness in humans and Nagana in domestic animals (Keating *et al.*, 2015, Büscher *et*
4 *al.*, 2017). They are members of the family of Kinetoplastida, which includes other parasites such
5 as *Trypanosoma cruzi*, the causative agent of Chagas disease, and various species of *Leishmania*
6 that cause leishmaniases. These parasites all have complex life cycles that alternate between an
7 insect vector and the mammalian host. In *T. brucei*, two well studied life cycle stages are the
8 procyclic form (PF), which is found in the tsetse fly vector and the bloodstream form (BF), present
9 in the blood of the infected animal host (Matthews, 2005). *T. brucei* exhibits several unique
10 biological features, such as a condensed bipartite mitochondrial genome with its unique replication
11 machinery, uridine insertion/deletion RNA editing of mitochondrial mRNAs, as well as a complex
12 mechanism to evade the host immune system by frequent changes of variant surface glycoproteins
13 (Jensen & Englund, 2012, Verner *et al.*, 2015, Bangs, 2018, Zimmer *et al.*, 2018, Aphasizheva *et*
14 *al.*, 2020). The process of transcription in these parasites is also unusual. Most protein coding
15 genes are transcribed by RNA polymerase II to produce long polycistronic units which are co-
16 transcriptionally processed to monocistronic mRNAs. Individual mRNAs are produced by 5'
17 *trans*-splicing that adds a 39-nt long spliced leader RNA to the 5' end of each monocistronic RNA
18 and 3' addition of a poly(A) tail (Michaeli, 2011). Due to the absence of promoters upstream of
19 individual genes, gene regulation in *T. brucei* takes place primarily at the posttranscriptional level
20 (Clayton, 2019).

21
22 Posttranscriptional gene expression in eukaryotes involves multiple steps including processing of
23 nascent transcripts, nuclear export of mature mRNAs, and regulation of both mRNA decay and
24 translational efficiency. mRNA export machineries have been extensively studied in the model
25 organism *Saccharomyces cerevisiae* and later in metazoan species (Köhler & Hurt, 2007,
26 Wickramasinghe & Laskey, 2015). In the established universal model of mRNA export, pre-
27 mRNA is co-transcriptionally assembled to a messenger ribonucleoprotein (mRNP) by the TREX
28 complex, followed by mRNA processing and maturation. Adaptor proteins that exhibit RNA
29 binding activity recruit the heterodimeric export receptor Mex67/Mtr2 to the mRNP and promote
30 export through the nuclear pore complex (NPC) (Tutucci & Stutz, 2011). In trypanosomes,
31 homologues of Mex67 and Mtr2 interact and function as nuclear export receptors for both mRNA

1 and tRNA (Schwede *et al.*, 2009, Dostalova *et al.*, 2013, Hegedúsová *et al.*, 2019). Nevertheless,
2 the domain organization of Mex67 in *T. brucei* is quite different than that of its yeast and metazoan
3 orthologues. Like yeast or metazoan Mex67, *T. brucei* Mex67 contains both leucine-rich repeat
4 (LRR) and an NTF2-like domains; however, it lacks an RNA recognition motif (RRM) and a
5 ubiquitin-associated domain (UBA) (Dostalova *et al.*, 2013, Rink & Williams, 2019). Moreover,
6 *T. brucei* Mex67 contains a CCCH zinc finger (ZC3H) motif in its N-terminal region, which is
7 essential for mRNA export (Dostalova *et al.*, 2013). Other aspects of the nuclear export machinery
8 also differ in *T. brucei* compared to other well studied systems. Unlike yeast or metazoans,
9 trypanosomatids contain no recognizable components of the TREX complex, with the exception
10 of the DEAD box helicase, Sub2 (Serpeloni *et al.*, 2011a, Dostalova *et al.*, 2013). Recent studies
11 suggest that active transcription is necessary to initiate mRNA export in *T. brucei*, although neither
12 the completion of transcription nor splicing appear to be essential for export (Goos *et al.*, 2018).

13

14 RNA binding proteins (RBPs) play major roles in gene expression and development in
15 trypanosomes. In some cases, RBPs have been shown to bind specific *cis*-acting regulatory
16 elements present in the 3'-untranslated regions (3'-UTRs) of mRNAs to modulate mRNA stability
17 or translation (Kolev *et al.*, 2014, Clayton, 2019). RBPs are classified into different groups based
18 on the presence of distinct RNA binding domains, with RNA recognition motif (RRM) and ZC3H-
19 containing proteins being the most common RBPs in trypanosomes (Kolev *et al.*, 2014). Examples
20 of the impacts of RBPs in *T. brucei* include the critical roles in developmental gene regulation
21 played by RRM-containing RBPs, RBP10 and RBP6, and REG9.1 (Kolev *et al.*, 2012, Mugo &
22 Clayton, 2017, Rico *et al.*, 2017). With regard to ZC3H proteins, ZC3H11 mediates gene
23 expression during heat shock (Droll *et al.*, 2013), and ZC3H20 binds specifically to a subset of
24 mRNAs expressed in PFs (Liu *et al.*, 2020).

25

26 DRBD18 is an essential and abundant an RRM-containing RBP in *T. brucei* (Lott *et al.*, 2015).
27 Our previous studies demonstrated that depletion of DRBD18 causes extensive transcriptome
28 rearrangement in PF *T. brucei* through both stabilization or destabilization of distinct subsets of
29 mRNAs. The molecular functions of DRBD18 in mRNA stabilization or destabilization and
30 protein-protein interactions are markedly controlled by methylation of arginine residues present
31 between its two RRM domains. Towards an understanding of the biochemical mechanisms of

1 DRBD18 function, mass spectrometry analysis of Tandem Affinity Purified (TAP)-tagged
2 DRBD18 revealed the interaction of DRBD18 with numerous proteins involved in RNA biology,
3 including the general mRNA export receptors Mex67 and Mtr2, and the Sub2 RNA helicase (Lott
4 *et al.*, 2015). Previous immunofluorescence analysis revealed a strong perinuclear concentration
5 of DRBD18 that, together with its interaction with Mex67/Mtr2, is consistent with a role for
6 DRBD18 in nucleocytoplasmic mRNA transport (Lott *et al.*, 2015). In the present study, we confirm
7 the *in vivo* association between DRBD18 and Mex67/Mtr2 and demonstrate that DRBD18 and
8 Mtr2 directly interact *in vitro*. High throughput sequencing and immunofluorescence studies show
9 that DRBD18 promotes the export of a subset of mRNAs from nucleus to cytosol. At the same
10 time, DRBD18 also facilitates the export of a fraction of Mex67/Mtr2 from the nucleus. In contrast,
11 DRBD18 does not share a function with Mex67/Mtr2 in the export of intron-containing or mature
12 tRNAs. The mRNA export machinery is not well characterized in *T. brucei* due to the absence of
13 many conserved export factors. The current study is the first to document a *T. brucei* RBP that
14 targets the mRNA export machinery.

15

16 **2 RESULTS**

17 ***2.1 DRBD18 interacts with export receptor proteins Mex67 and Mtr2 in vivo***

18 Our previous mass spectrometry analysis suggested that DRBD18 associates with several RNA
19 processing complexes, including the nuclear export factors, Mex67 and Mtr2 (Lott *et al.*, 2015).
20 These two factors are evolutionarily conserved and typically form a heterodimer, although distinct
21 functions for Mex67 and Mtr2 have also been reported (Braun *et al.*, 2002, Dostalova *et al.*, 2013,
22 Hegedúsová *et al.*, 2019). To explore whether DRBD18 plays a role in Mex67/Mtr2 mediated
23 RNA export, we began by confirming the interactions of Mex67 and Mtr2 with DRBD18 *in vivo*.
24 For this purpose, we generated PF *T. brucei* cells expressing HA-tagged Mtr2 from its genomic
25 locus. Immunoprecipitation (IP) using anti-HA antibody in the aforementioned cell line confirmed
26 that Mtr2 associates with DRBD18, as well as with Mex67 as expected, while both are absent in a
27 control IP (Fig. 1A). As DRBD18 is an RNA binding protein (Lott *et al.*, 2015), we next asked
28 whether the DRBD18-Mtr2 interaction is impacted by RNA by performing co-IPs using HA-Mtr2
29 tagged *T. brucei* cell lysate treated either with an RNase cocktail or with RNase inhibitor (Figs.
30 1B and 1C). DRBD18 consistently displayed an increased interaction with Mtr2 in the absence of
31 RNA, whereas the interaction between Mex67 and Mtr2 was unaffected by RNA. To further probe

1 the RNA dependence of DRBD18-Mex67/Mtr2 interaction, we immunoprecipitated DRBD18
2 with anti-DRBD18 antibody from the HA-Mtr2 tagged *T. brucei* cell lysate in presence and
3 absence of RNase, and demonstrated increased co-immunoprecipitation of both Mex67 and Mtr2
4 with DRBD18 in RNase treated samples (Figs. 1D and 1E). Thus, we conclude that DRBD18
5 associates with Mex67/Mtr2 *in vivo*, and that this interaction is strengthened in the absence of
6 RNA.

7 8 **2.2 DRBD18 directly interacts with Mtr2 in vitro**

9 Having demonstrated the *in vivo* DRBD18-Mex67/Mtr2 interaction, we next asked if DRBD18
10 interacts directly with the export receptors. To this end, we expressed and purified recombinant
11 His-Mtr2, GST-DRBD18, and GST in *E. coli* as described in Experimental Procedures. Purity of
12 the recombinant proteins was analyzed by SDS-PAGE analysis (Fig. 2A). Next, we performed
13 GST-pulldown assays using GST-DRBD18 as bait protein, GST as a negative control, and purified
14 His-Mtr2 as prey protein. For this purpose, we incubated equimolar amounts of purified His-tagged
15 Mtr2 with the immobilized GST or GST-DRBD18. Western blot analysis showed that Mtr2 is
16 pulled down by the GST-tagged DRBD18 but not by GST, indicating that DRBD18 interacts
17 directly with Mtr2 (Fig. 2B). These data collectively demonstrate that DRBD18 interacts with
18 Mtr2 through a protein-protein interaction.

19 20 **2.3 DRBD18 does not impact Mex67/Mtr2-dependent export of tRNAs**

21 To begin to understand the functional significance of the DRBD18-Mex67/Mtr2 interaction, we
22 first confirmed that DRBD18 does not alter the steady state levels or heterodimerization of Mex67
23 and Mtr2 (Fig. S1). As these parameters are unaffected by DRBD18 knockdown, the interaction
24 between DRBD18 and Mex67/Mtr2 suggests that DRBD18 could impact some functions of these
25 export factors. It was recently reported that Mex67 and Mtr2 play important and distinct roles in
26 tRNA nuclear export in *T. brucei* (Hegedúsová *et al.*, 2019). Knockdown of Mtr2 results in nuclear
27 accumulation of all type of tRNAs, while Mex67 knockdown leads to nuclear accumulation of
28 subsets of tRNAs that are modified with queuosine. To investigate the functional role of the
29 DRBD18-Mex67/Mtr2 interaction in tRNA export, we analyzed total RNA from uninduced and
30 induced DRBD18 RNAi cells by Northern hybridization. We first monitored the splicing of
31 tRNA^{Tyr}, which occurs exclusively in the cytosol in *T. brucei* and, thus, serves as a measure of the

1 export of immature, intron-containing tRNA^{Tyr}. We observed no effect of DRBD18 knockdown
2 on this parameter, similar to the lack of Mex67 or Mtr2 impact on export of this immature tRNA
3 (Fig. S2). Following splicing, tRNA^{Tyr} undergoes retrograde import into the nucleus, at which
4 point it acquires a queuosine modification and is then re-exported. Impairment of this re-export
5 step, which requires both Mex67 and Mtr2, results in aberrantly high queuosine levels on tRNA^{Tyr}
6 (Hegedúsová *et al.*, 2019). We next asked whether DRBD18 exerts any modulation of the function
7 of Mex67 and Mtr2 in the re-export of tRNA^{Tyr} by analyzing the level of queuosine modified
8 tRNA^{Tyr} using boronate affinity gel electrophoresis followed by Northern blot hybridization
9 (Kessler *et al.*, 2018). RNA samples treated with the oxidizing agent, sodium periodate, served as
10 a negative control (Fig. 3A). We detected similar levels of queuosine modified tRNA^{Tyr} in RNA
11 from uninduced and induced DRBD18 RNAi cells (Fig. 3A), indicating that DRBD18 does not
12 impact the Mex67/Mtr2 mediated re-export of queuosine modified tRNA^{Tyr}. To further investigate
13 the potential role of DRBD18 in tRNA export, we analyzed mature tRNA^{Tyr} and tRNA^{Glu} (Figs.
14 3B and 3C) by fluorescence *in situ* hybridization (FISH) using specific fluorophore labeled
15 oligonucleotide probes (Table S1). These probes detect spliced tRNA, regardless of its queuosine
16 modification status. Unlike what is observed in Mtr2 or Mex67 knockdowns, we did not observe
17 any nuclear accumulation of mature tRNA^{Tyr} or tRNA^{Glu} when DRBD18 is knocked down.
18 Collectively, these data show that DRBD18 does not impact the functions of Mex67 or Mtr2 with
19 respect to their roles in the export or re-export of tRNAs.

20

21 **2.5 DRBD18 plays role in mRNA export from nucleus to cytosol**

22 Mex67/Mtr2 plays an important role in mRNA transport from nucleus to cytosol in *T. brucei*
23 (Dostalova *et al.*, 2013), but the mechanisms of export are poorly understood. The interaction of
24 DRBD18 with these export factors (Figs. 1 and 2) suggests that DRBD18 could modulate export
25 of at least some mRNAs. To determine whether DRBD18 exerts any functional role on mRNA
26 export from nucleus to cytosol, we first assessed the subcellular location of poly(A)⁺ RNA in
27 DRBD18 RNAi uninduced and induced cells by oligo(dT) FISH (Fig. 4A). To quantify the mRNA
28 distribution in the nucleus, we plotted the fluorescence intensities of the FISH and DAPI signals
29 across the nucleus, with overhangs covering the cytosol, across multiple cells (Fig. 4B). In
30 DRBD18 RNAi induced cells, we observed substantial overlap between FISH signals and DAPI
31 signals (lower panel), while uninduced cells exhibited minimum overlap between two fluorophores

1 (upper panel). These observations demonstrate that DRBD18 depletion causes partial
2 accumulation of mRNA in nucleus, thereby indicating a role for DRBD18 in export of mature
3 mRNA from nucleus to cytosol.

4 5 **2.6 DRBD18 regulates gene expression by promoting the export of a subset of mRNAs**

6 The partial nuclear retention of mRNA in DRBD18 depleted cells (Fig. 4) suggests that DRBD18
7 impacts nuclear export of only a subset of mRNAs. To identify a cohort of mRNAs whose export
8 is affected by DRBD18, we carried out Illumina NextSeq analysis of total RNA and cytosolic
9 RNA from uninduced and induced DRBD18 RNAi cells. We identified mRNAs whose abundance
10 is unchanged in whole cell RNA, but decreased in cytosolic RNA upon DRBD18 RNAi, as an
11 indication of decreased nuclear export (Müller-McNicoll *et al.*, 2016, Rehwinkel *et al.*, 2004,
12 Wickramasinghe *et al.*, 2014). The purity of subcellular fractionation and the depletion of
13 DRBD18 by RNAi induction were confirmed by Western blot analysis using antibodies against
14 cytosolic and nuclear marker proteins and anti-DRBD18 antibody, respectively (Fig. S3). In whole
15 cell RNA, we identified 259 transcripts that decreased in abundance and 378 that increased upon
16 DRBD18 knockdown (1.5 fold change; corrected p-value <0.05) (Table S2), similar to our
17 previously published findings (Lott *et al.*, 2015). In the cytosolic fraction, we identified 216
18 transcripts with decreased abundance and 593 transcripts with increased abundance (1.5 fold
19 change; corrected p-value <0.05) upon DRBD18 knockdown (Table S3, Fig. S4). Next, we
20 focused on the set of transcripts whose nuclear export was apparently promoted by DRBD18,
21 consistent with the partial nuclear accumulation of poly(A)⁺ RNA that we observed by FISH (Fig.
22 5). To this end, we identified mRNAs reduced in cytosol and unchanged in the whole cell upon
23 DRBD18 RNAi (Fig. 5A; Fig. S4). Of the 174 transcripts fitting these parameters (corrected p-
24 value <0.05; Fig. 5A), 95 exhibited a fold decrease in the cytosol of >1.5 fold (Fig. 5A, blue).
25 These 95 transcripts comprise the list of potential DRBD18 facilitated export targets (Table S4).
26 No significantly enriched GO terms or nucleotide motifs were apparent in this mRNA set. To
27 validate the relative expression of the transcripts in cytosol and whole cell in DRBD18 RNAi
28 induced or uninduced cells, we performed qRT-PCR analyses on a subset of these transcripts. By
29 qRT-PCR, we detected either no decrease or small decreases in the transcripts in whole cell RNA
30 samples as expected (Figs. 5B and S5), and we confirmed significantly larger decreases in the
31 cytosol for seven of the transcripts tested (Fig. 5B). An additional four transcripts showed no

1 significant differences between whole cell and cytosol, although some appeared to trend in this
2 direction (Fig. S5). If the nuclear export of these transcripts is directly promoted by DRBD18,
3 we would expect them to associate with DRBD18 *in vivo*. To test this, we performed cross-linking
4 immunoprecipitation (CLIP) experiments in which we measured the enrichment of the transcripts
5 in Fig. 5B using anti-DRBD18 antibodies relative to a non-specific antibody control. Indeed, all
6 seven transcripts were enriched, from 2- to 17-fold, while a negative control transcript
7 (Tb927.7.7400; Table S2) was not (Fig. 5C). The reduced abundance of specific mRNAs in cytosol
8 compared to that in the whole cell RNA population upon DRBD18 depletion is consistent with a
9 function for DRBD18 in the export of these mRNAs. Moreover, DRBD18 binds differentially
10 transported mRNAs *in vivo*, suggesting it plays a direct role in promoting the nucleocytoplasmic
11 transport of a subset of mRNAs.

12

13 ***2.7 DRBD18 levels impact the relative abundance of export receptors in nucleus and cytosol*** 14 ***mRNA***

15 One mechanism by which DRBD18 may promote export of selected mRNAs is by facilitating the
16 nuclear export of the Mex67/Mtr2-DRBD18 mRNP. To determine whether DRBD18 impacts the
17 transport of Mex67/Mtr2 from nucleus to cytosol, we fractionated DRBD18 RNAi induced and
18 uninduced cells into nuclear and cytosolic fractions, and validated the fractionation by western
19 blot analysis of histone H3 and EF1 α , respectively (Figs. 6A and 6B). We then blotted for Mex67
20 and Mtr2 in both fractions and normalized their expression to the expression of histone H3
21 (nucleus) or EF1 α (cytosol). We detected a significant and reproducible approximately two-fold
22 increase in nuclear Mex67 and Mtr2 in cells depleted of DRBD18. We did not detect significant
23 concomitant changes in Mtr2 or Mex67 level in cytosolic fraction of DRBD18 RNAi induced and
24 uninduced cells, possibly due to the greater abundance of Mex67/Mtr2 in the cytosol in our assay
25 system. These data indicate that DRBD18 modestly impacts the dynamics of export receptor
26 trafficking between the two subcellular compartments, consistent with its ability to promote the
27 export of a subset of mRNAs.

28

29 **3 DISCUSSION**

30 Gene expression in kinetoplastids, including *T. brucei*, is modulated primarily at the
31 posttranscriptional level, with RBPs constituting the key gene regulatory factors (Clayton, 2019).

1 While RBPs and *cis*-acting sequences that modulate mRNA stability and translation have been
2 identified in *T. brucei*, no proteins outside the basal nuclear export machinery have been reported
3 to control mRNA export (Schwede *et al.*, 2009, Dostalova *et al.*, 2013). Here, we show that the
4 abundant and essential *T. brucei* RBP, DRBD18, promotes the nucleocytoplasmic transport of a
5 subset of mRNAs. While nuclear mRNA export was originally thought to be constitutive, more
6 recent studies reveal that nuclear export of mRNAs can be highly selective, and this process is now
7 established as an important level of gene regulation (Wickramasinghe & Laskey, 2015). In
8 mammals, processes such as DNA repair, maintenance of pluripotency, stress responses, and cell
9 proliferation can be regulated by selective nuclear export promoted by distinct proteins. We
10 demonstrate here that *T. brucei* DRBD18 binds the general nuclear export receptor, Mex67/Mtr2,
11 likely through a direct interaction with Mtr2, and facilitates the export of a subset of mRNAs.
12 Thus, DRBD18 is the first reported nuclear mRNA export specificity factor in trypanosomes.

13

14 Bulk nuclear mRNA export is facilitated in yeast and mammals by the TREX complex,
15 which binds to Mex67 and increases its affinity for mRNA. With the exception of the Sub2 RNA
16 helicase, homologues of TREX complex components are absent in *T. brucei* (Serpeloni *et al.*,
17 2011b); however, DRBD18 clearly does not fulfill the bulk export role of a TREX component, as
18 it impacts the export of only a few hundred mRNAs. Indeed, it has been suggested that *T. brucei*
19 Mex67 may not utilize a homolog of the TREX complex to increase bulk mRNA binding due to
20 the presence of a kinetoplastid-specific ZC3H domain at its N terminus (Dostalova *et al.*, 2013).
21 DRBD18 may act as an adaptor protein that promotes association of a select subset of mRNAs
22 with Mex67/Mtr2. Alternatively, or in addition, DRBD18 may function as a nuclear export
23 chaperone. The nuclear envelope defines the physical barrier between nucleoplasm and cytosol,
24 and communication between the two compartments is mediated by cylindrical macromolecular
25 NPCs. Rate limiting steps in mRNA nuclear export are diffusion of mRNA loaded Mex67/Mtr2
26 through the nucleoplasm and loading onto NPC, the latter of which requires the activity of
27 chaperones that direct cargo to the NPC (Scott *et al.*, 2019). Chaperoning of Mex67/Mtr2 to the
28 NPC has been proposed as a good target for regulation of the export rate of specific subsets of
29 mRNAs (Scott *et al.*, 2019).

30

1 One clue as to how DRBD18 might facilitate export of mRNAs bound by the Mex67/Mtr2-
2 DRBD18 mRNP lies in the reported interactions of Mex67 and DRBD18 with NPC components.
3 The NPC consist of multiple copies of ~30 proteins termed nucleoporins (Nups), of which *T.*
4 *brucei* contains two major classes: phenylalanine-glycine (FG) repeats Nups and core scaffold
5 Nups (Fig. 7) (Obado *et al.*, 2016). The core scaffold, which is comprised of two inner ring and
6 two outer ring structural components interacts with the nuclear envelope. FG Nups are disordered
7 proteins responsible for the selective permeability of the NPC to nucleocytosolic transport, playing
8 vital roles in the transport of the soluble transport receptors through hydrophobic interactions
9 (Strambio-De-Castillia *et al.*, 2010). Comprehensive proteomic and interactome analysis of *T.*
10 *brucei* NPC by Obado, *et al.* (Obado *et al.*, 2016) revealed both similarities and differences in the
11 NPC protein composition in this excavate compared to that of the opisthokonts (humans and yeast).
12 Further, affinity capture of *T. brucei* Mex67 revealed its association with many components of the
13 NPC (Obado *et al.*, 2016). Under high stringency, Mex67 interactions were observed
14 predominantly with the less evolutionarily conserved outer ring and FG Nups. In particular, the
15 retention of FG Nups comprising the Nup76 complex (Nups 76, 140, and 149; see Fig. 7) under
16 high stringency implicates the Nup76 complex as part of the mRNA export docking platform.
17 Previous Tandem Affinity Purification (TAP) of DRBD18-TAP from PF *T. brucei* also returned
18 several NPC components (Lott *et al.*, 2015). Remarkably, these studies identified as DRBD18
19 interacting NPC proteins almost exclusively those that also showed high stringency interactions
20 with Mex67, including components of the Nup76 complex (Nups140 and 149) and the outer ring
21 (Nups 158, 132, 109, 89, and 82). Interaction of DRBD18 with the Nup76 complex docking
22 platform may increase the frequency and/or affinity with which the Mex67/Mtr2 complex interacts
23 with the NPC, thereby facilitating export of mRNAs bound to the Mex67/Mtr2-DRBD18 complex
24 (Tetenbaum-Novatt & Rout, 2010). Future studies will be needed to address the precise mechanism
25 by which DRBD18 promotes the export of a distinct mRNA subset.

26
27 While DRBD18 clearly facilitates the export of a subset of mRNAs as described here, we
28 also identified numerous mRNAs whose export may be inhibited by DRBD18. Over 500 mRNAs
29 are increased in the cytosol upon DRBD18 knockdown, and approximately 200 of these mRNAs
30 are not increased in whole cell RNA pools (Fig. S4). Thus, it is likely that DRBD18 has dual and
31 opposing roles in mRNA nuclear export. In model organisms, posttranslational modifications of

1 the nuclear export machinery impact numerous steps in this process (Tutucci & Stutz, 2011,
2 Howard & Sanford, 2015, Wickramasinghe & Laskey, 2015). One potential mechanism for
3 regulation of disparate functions of DRBD18 in mRNA export in *T. brucei* is the methylation of
4 arginine residues that lie between the two DRBD18 RRM domains (Lott *et al.*, 2015). We
5 previously demonstrated that arginine methylation promotes the ability of DRBD18 to stabilize
6 mRNAs, while it inhibits the DRBD18 mediated destabilization of other transcripts. With regard
7 to Mex67/Mtr2, DRBD18 TAP returned increased numbers of Mex67 peptides with
8 hypomethylated DRBD18, but increased Mtr2 peptides with methylmimic DRBD18, so the impact
9 of methylation on the DRBD18-Mex67/Mtr2 interaction is unresolved. Additionally, with a few
10 exceptions, most Nups appeared to bind equivalently to hypomethylated and methylmimic
11 DRBD18 (Lott *et al.*, 2015). It has been suggested that selective mRNA nuclear export in mammals
12 is controlled by combinatorial binding of distinct RBP combinations to a given transcript
13 (Wickramasinghe & Laskey, 2015). Interestingly, TAP of hypomethylated and methylmimic
14 DRBD18 identified several RRM and ZC3H RBPs that were differentially bound to DRBD18 in
15 RNase-treated extracts depending on its methylation status (Lott *et al.*, 2015). This finding
16 suggests that these DRBD18 associated RBPs could contribute to a combinatorial effect on nuclear
17 mRNA export in *T. brucei* with distinct impacts based on the methylation status of DRBD18.

18
19 Nuclear mRNA export interfaces with other RNA processing and gene regulatory events
20 (Howard & Sanford, 2015, Wickramasinghe & Laskey, 2015). One such process is nuclear mRNA
21 decay. Nuclear retained mRNAs are generally turned over, and the balance between mRNA export
22 kinetics and decay can be a key determinant of gene expression (Meola & Jensen, 2017, Tudek *et*
23 *al.*, 2019). In yeast, experimental inhibition of nuclear export leads to the degradation of protein
24 coding transcripts (Tudek *et al.*, 2018). In light of these findings, our approach to identifying
25 transcripts whose nuclear export is promoted by DRBD18 may have been conservative. Because
26 we identified only those mRNAs whose abundance was statistically unchanged in the whole cell
27 RNA pool, but decreased in cytosol, we would not have identified those mRNAs whose abundance
28 was significantly decreased by decay upon nuclear retention. Thus, the impact of DRBD18 in
29 promoting mRNA export may be broader than reported here. Nuclear mRNA export can also be
30 coupled to transcript specific translation by nucleocytoplasmic shuttling proteins, such as some SR
31 proteins (Maslon *et al.*, 2014, Howard & Sanford, 2015, Brugiolo *et al.*, 2017). DRBD18 localizes

1 to both nucleus and cytosol, with a perinuclear concentration (Fig. S3) (Lott *et al.*, 2015). This
2 localization pattern, together with its interaction with numerous NPC components, suggests that
3 DRBD18 may undergo nucleocytoplasmic shuttling. Interestingly, DRBD18-TAP purification
4 revealed the protein's interaction with ribosomes and translation initiation factors (Lott *et al.*,
5 2015). In addition, Klein, *et al.* reported association of DRBD18 with bloodstream form *T. brucei*
6 polysomes (Klein *et al.*, 2015). Thus, one possible scenario entails sequence specific coupling of
7 mRNA nuclear export and translation by DRBD18 to enhance gene expression. Together, our data
8 suggest that DRBD18 is a multifunctional gene regulatory protein with the potential to integrate
9 mRNA export, stability, and translation.

10

11 **4 EXPERIMENTAL PROCEDURES**

12

13 **4.1 Cell line generation and culture**

14 PF *T. brucei* strain 29-13 and all cell lines derived from this strain were grown at 27°C in SM
15 medium supplemented with 10% fetal bovine serum and containing hygromycin (50µg ml⁻¹) and
16 G418 (15µg ml⁻¹). Cells harboring the doxycycline inducible DRBD18 (Tb927.11.14090) RNA
17 interference (RNAi) constructs described previously in (Lott *et al.*, 2015) were grown with the
18 addition of phleomycin (2.5µg ml⁻¹). To induce RNAi, the clonal cell line was incubated for 19 h
19 (high throughput sequencing and qRT-PCR) or 23 h (all other experiments) with 4µg ml⁻¹
20 doxycycline. *In situ* tagging of *TbMtr2* with a triple hemagglutinin (3XHA) tag was performed by
21 the long primer PCR method, using the pPOTv6 plasmid according to the published protocol by
22 (Dean *et al.*, 2015). Primers are listed in Table S1. PCR products were transfected into *T. brucei*
23 for genomic integration, and transfectants were selected with blasticidin (20µg ml⁻¹).

24

25 **4.2 Immunoprecipitation and Western blot**

26 Approximately 1.5 X 10⁹ cells were collected, washed with PBS, and resuspended in lysis buffer
27 (50 mM HEPES (pH 7.4), 3 mM MgCl₂, 150 mM KCl, 150 mM sucrose, 0.5% Tween-20, EDTA-
28 free protease inhibitor cocktail (Roche, USA), and 1mM DTT). Cells were lysed by sonication
29 (Sonic Dismembrator, Fisher Scientific, USA) three times for 15s at 30s intervals on ice at 60%
30 amplitude, and clarified by centrifugation at 15,000xg for 30 min at 4°C. For immunoprecipitation
31 with anti-HA antibody, clarified lysates were incubated with agarose immobilized rabbit anti-HA
32 beads (ICL Laboratories, USA) for 2 h at 4°C. As a negative control, lysates were incubated with

1 IgG Sepharose beads (GE Healthcare, USA) for 2 h at 4°C. Bound proteins were eluted with 100
2 mM glycine (pH 2.5) and the solution neutralized using 1M Tris buffer (pH 7.5). Proteins were
3 electrophoresed on a 12.5% SDS-PAGE gel and transferred to nitrocellulose membrane.
4 Membranes were blocked with 5% non-fat dry milk in Tris buffered saline with Tween-20 (TBST)
5 and probed with polyclonal antibodies against DRBD18 (Lott *et al.*, 2015), p22 (Hayman *et al.*,
6 2001) and Mex67 (a kind gift from Prof. Mark Carrington, University of Cambridge, UK).
7 Commercially available antibodies against HA-epitope (Mouse monoclonal, Thermo Fisher
8 Scientific), Histone H3 (Rabbit polyclonal, Abcam), and EF1 α (Mouse monoclonal, Santa Cruz
9 Biotechnology) were also used. Blots were washed with TBST and subsequently probed with
10 secondary antibodies, either goat anti-rabbit HRP or goat anti-mouse HRP. Signals were detected
11 using an ECL preparation as recommended by the manufacturer (Thermo Fisher Scientific, USA),
12 visualized on a Chemi Doc MP imaging system (BioRad), and quantified using BioRad Image Lab
13 software.

14

15 **4.3 Protein expression and GST pulldown assay**

16 Expression of recombinant GST-tagged DRBD18 was carried out as described earlier (Lott *et al.*,
17 2015). For His-Mtr2 (Tb927.7.5760), the ORF was cloned into the MCS-1 of pETDuet-1 vector
18 (with MSC2 left empty), with frame shift correction by insertion of single nucleotide before the
19 start codon (Kafková *et al.*, 2017) and was purified using immobilized metal affinity
20 chromatography (IMAC) as described earlier (Klebanov-Akopyan *et al.*, 2018). For GST pulldown
21 assays, all recombinant plasmids including pGEX4T-1, were transformed into *Escherichia*
22 *coli* BL21 strain, and protein expression was induced by addition of 0.5 mM isopropyl 1-thio-D-
23 galactopyranoside (IPTG) and subsequent growth at 22°C overnight. Cells expressing GST-
24 DRBD18 or GST were harvested and resuspended in lysis buffer (50 mM Tris-HCl (pH 8.0), 250
25 mM NaCl, 5 mM EDTA, 10 mM DTT, and 1mM PMSF) and lysed by four cycles of maximum-
26 power sonication bursts of 30 s each at 4°C. Triton X-100 was added to a final concentration of
27 1%, followed by a 30 min centrifugation at 15,000 xg and 4°C. The supernatant was incubated
28 with Glutathione-Sepharose 4B beads (GE) at 4°C for 2 h. The column was extensively washed
29 with ice cold lysis buffer. Equal amounts of purified His-Mtr2 were added and incubated for
30 another 2 h at 4°C with the immobilized GST or GST fusion protein. The columns were
31 washed with ice cold wash buffer. The beads were boiled with SDS-PAGE Laemmli buffer

1 and analyzed by Western blot using anti-Histidine (anti-Mouse, Sigma Aldrich) and anti-GST
2 antibodies (anti-Rabbit, Sigma Aldrich).

3

4 **4.4 RNA isolation from nuclear-cytosolic fractionation**

5 Nuclear-cytosolic fractionation was performed in triplicate as described previously in Dostalova,
6 *et al.* (Dostalova *et al.*, 2013). Briefly, 2.5×10^8 PF cells were harvested, washed in phosphate
7 buffer saline (PBS), and resuspended in PBS. Nonidet-P40 was added to final concentration of
8 0.1%, the cell suspension was mixed thoroughly, and nuclei were pelleted by centrifugation at
9 2300xg for 1 min. Supernatant was considered as cytosolic fraction. To validate the fractionation
10 and DRBD18 knockdown, samples corresponding to same cell equivalents from whole cells and
11 supernatant (cytosolic) fractions were subjected to SDS-PAGE and Western blot analysis with
12 anti-DRBD18, anti-histone H3, and anti-EF1 α antibodies. For RNA isolation, Trizol reagent
13 (Invitrogen) was added to the cytosolic fraction and this suspension frozen at -80°C. Total RNA
14 was isolated from whole cell and cytosolic fractions using Trizol reagent and phenol chloroform
15 extraction followed by DNase-I treatment (DNA-free DNase kit; Ambion). The RNA was further
16 purified using phenol chloroform extraction. Purified RNA samples were submitted for RNA
17 sequencing and also kept for qRT-PCR analysis.

18

19 **4.5 RNA library preparation, sequencing, and bioinformatic analysis**

20 Prior to library preparation, total RNA was quality checked using an Agilent Fragment Analyzer
21 to assess quality and Qubit Fluorescence (Invitrogen) to measure concentration. RNA libraries
22 were prepared following the New England Biolabs NEXT UltraII Directional RNA library kit
23 using polyA⁺ magnetic beads. Following library preparation, concentration and quality control,
24 final libraries were pooled to 10 nM and the concentration of the pool was determined using the
25 Kapa Biosystems Universal qPCR kit. After dilution and denaturing, the pooled library was loaded
26 onto a NextSeq 500 high output flow cell (PE75) for sequencing. Sequencing quality was assessed
27 using FastQC and MultiQC, and low-quality bases were removed using TrimGalore, a cutadapt
28 wrapper (Andrews, 2010, Krueger, 2015, Ewels *et al.*, 2016, Martin, 2011). Ribosomal RNA
29 (rRNA) reads were removed with SortMeRNA prior to alignment with Spliced Transcripts
30 Alignment to a Reference (STAR) against the TREU927 *T. brucei* reference genome, downloaded
31 from TriTrypDB v41 (Kopylova *et al.*, 2012, Dobin *et al.*, 2013, Aslett *et al.*, 2010). Transcript

1 abundances were estimated with RNA-Seq by Expectation Maximization (RSEM) (Li & Dewey,
2 2011). Differential abundances were identified using differential expression analysis for sequence
3 count data (DESeq2) (Love *et al.*, 2014).

4
5 The sequencing data used in this study has been deposited in Sequence Read Archive, accession
6 number GSE158584.

7
8 **4.6 qRT-PCR analysis**

9 Reverse transcription (RT) was performed with 1 µg of DNase I-treated RNA following standard
10 procedures with random hexamer primers and iScript reverse transcriptase (BioRad). Quantitative
11 reverse transcription PCR (qRT-PCR) reactions were performed using primer pairs targeted at
12 specific transcripts (Table S1). Amplification was performed using a CFX Connect Real Time
13 System (Bio Rad), and data were analyzed using BioRad CFX Manager 3.1. Results were analyzed
14 using the Bio-Rad CFX Manager 3.1 software. RNA levels were normalized to 18S rRNA using
15 the standard curve method.

16
17 **4.7 Fluorescence *in situ* hybridization (FISH)**

18 For tRNA FISH analysis, cells were harvested, fixed and permeabilized as described (Hegedúsová
19 *et al.*, 2019) and then pre-hybridized for 2h with hybridization solution (2% BSA, 5X Denhardt's
20 solution, 4X SSC, 5% dextran sulphate, 35% deionized formamide, 10 U ml⁻¹ RNase inhibitor).
21 The slides were then incubated overnight at room temperature in a humid chamber in the presence
22 of 10 ng µl⁻¹ fluorophore labeled oligonucleotide probes (Supplementary Table S1), in the
23 hybridization solution. Slides were washed as described earlier (Hegedúsová *et al.*, 2019) and
24 mounted with mounting medium supplemented DAPI. Images were taken with confocal
25 microscope Olympus Fluo ViewTM FV1000.

26
27 mRNA FISH analysis was performed as previously described (Dostalova *et al.*, 2013). Briefly, 2.5
28 X 10⁷ cells were harvested by centrifugation, washed, resuspended in PBS, and allowed to adhere
29 to poly-L-lysine coated slides for 30 min. Cells were fixed with 4% paraformaldehyde followed
30 by a 10 min treatment with 25mM ammonium chloride. Fixed cells were permeabilized for 1 h in
31 blocking buffer (PBS containing 0.5% saponin, 2% BSA and 10U ml⁻¹ RNase inhibitor).

1 Permeable cells were pre-hybridized for 2 h with hybridization solution (2% BSA, 5X Denhardt's
2 solution, 4X SSC, 5% dextran sulphate, 35% formamide, 0.5 $\mu\text{g } \mu\text{l}^{-1}$ tRNA, 10 U ml^{-1} RNase
3 inhibitor). Alexa 594-labelled oligo-(dT)₃₀ (2 ng μl^{-1} in hybridization solution; Invitrogen, USA)
4 was hybridized overnight at room temperature. Slides were then washed for 10 min, once with
5 50 μl of 4X SSC with 35% formamide followed by one wash each with 2X SSC and 1X SSC.
6 Labelled cells were mounted with 4',6-diamino-2-phenylindole dihydrochloride (DAPI)
7 fluoromount-G (Southern Biotech, Birmingham, AL) for visualization. Images were taken with a
8 fluorescent microscope Zeiss Axioimager M2 stand equipped with a rear-mounted excitation filter
9 wheel. mRNA FISH data were quantified using ImageJ (NIH) software as described previously
10 (Chatterjee *et al.*, 2017). Six cells (three from each replicate) were randomly selected and their
11 fluorescence intensities were measured using Image J with a plot profile analysis of the various
12 points at a regular interval along a line drawn across the nucleus with overhangs covering the
13 cytosol (Hegedúsová *et al.*, 2019). The results are expressed as the average value of relative
14 fluorescence intensity \pm S.D.

15

16 **4.8 Denaturing gel electrophoresis and Northern hybridization**

17 Total RNA was isolated using Trizol reagent and phenol chloroform extraction method as
18 described previously (Lott *et al.*, 2015). Boronate affinity electrophoresis was performed as
19 described previously (Kessler *et al.*, 2018). In brief, 5 μg of RNA was resolved by denaturing gel
20 electrophoresis (8% acrylamide, 7 M urea), electroblotted to Zeta probe[®] (Bio-Rad) membranes,
21 and UV cross-linked (1200 uJ \times 100). Oxidation control RNA was deacylated and treated with
22 sodium periodate and then the reaction was quenched by addition of 2.5 mM glucose. The
23 membranes were probed with oligonucleotides radiolabeled with γ ³² P-dATP (Supplementary
24 Table S1). Northern hybridization was performed according to the manufacturer's instructions
25 (Bio-Rad). Subsequently, the membranes were exposed overnight to a Phosphorimager screen and
26 analyzed using Typhoon[™] 9410 scanner and Image Quant TL software (GE Healthcare)
27 (Hegedúsová *et al.*, 2019).

28

29 **4.9 Cross-linking immunoprecipitation (CLIP)**

1 CLIP was carried out with minor modifications of a previously published method (Mugo & Erben,
2 2020). Briefly, procyclic form cells (1×10^7 cells ml^{-1}) were harvested and washed once with cold
3 1X PBS buffer (pH 7.4). Cells were resuspended in 25 ml of SM medium without FBS to a
4 concentration of $\sim 5 \times 10^9$ cells ml^{-1} , transferred to a 100 X 15 mm Petri dish, placed on ice, and UV
5 irradiated at 400 mJ/cm^2 in a Stratalinker 1800 (Stratagene). Cells were pelleted, washed with
6 PBS, snap frozen in liquid N_2 , and stored in -80°C until use. Cells were resuspended in 4 ml of
7 lysis buffer (Tris-HCl (pH 7.5), 150mM NaCl, 0.1 %NP40, and 1% Triton X-100) and then lysed
8 by passing 15–20 times through a 21 gauge needle. Cell lysate was cleared by centrifugation at
9 18000 rpm for 30 minutes at 4°C . Supernatant was collected, and the NaCl concentration adjusted
10 to 150 mM. Crosslinked DRBD18-RNA complexes were immunopurified from cellular extracts
11 using anti-DRBD18 antibodies (Lott *et al.*, 2015) attached to Protein A fast flow beads (GE
12 Healthcare); anti-Ty1 antibody attached to Protein A fast flow beads served as the control.
13 Captured protein-RNA complexes were washed with wash buffer (Tris-HCl (pH 7.5), 150mM
14 NaCl, 0.1 %NP40), and 5% of the beads were taken from each sample and used for Western blot
15 was performed to confirm the pulldown of DRBD18. Beads were treated with DNase 1 (Sigma)
16 followed by proteinase K (Roche). RNA was extracted with phenol/chloroform, and cDNA was
17 prepared using gene specific primers (Table S1) and qRT-PCR was performed as described above.
18 Fold change was calculated as described previously (McAdams *et al.*, 2018).

19

20

1 **FIGURE LEGENDS**

2

3 **Figure 1. DRBD18 interacts with the general export receptor proteins Mex67 and Mtr2 *in*** 4 ***vivo*.**

5 (A) Immunoprecipitations (IP) of *T. brucei* cells expressing 3XHA-tagged Mtr2 from its genomic
6 locus were carried out using anti-HA beads or IgG Sepharose beads (Control). Bound proteins
7 were eluted using 100 mM glycine and analyzed by Western blot with anti-HA, anti-DRBD18,
8 anti-Mex67, anti-Histone H3 (H3), and anti-EF1 α antibodies. Migration of molecular weight
9 standards (kDa) is indicated on the left. Two biological replicate experiments, each with two
10 technical replicates, were performed, and a representative experiment is shown. (B) HA-Mtr2 and
11 associated proteins were immunoprecipitated from *T. brucei* cell extracts that were treated with
12 either an RNase cocktail (+RNase) or RNase inhibitor (-RNase). Proteins were eluted and Western
13 blots performed as in (A). Two biological replicate experiments, each with two technical
14 replicates, were performed, and a representative experiment is shown. (C) Quantification of band
15 intensities of the experiment shown in (B). Protein levels were normalized to amount of HA-Mtr2
16 for a given IP. The normalized protein levels from the +RNase IP were then compared to that of
17 the -RNase IP (which was set to 1) to calculate the protein associated with HA-Mtr2. Bar graphs
18 represent the average and standard deviation (SD) of two biological replicates, each with two
19 technical replicates. (D) DRBD18 was immunoprecipitated from HA-Mtr2 expressing cells with
20 specific antibodies. Proteins were eluted and Western blots with anti-HA and anti-Mex67
21 antibodies were performed as in (A). Two biological replicate experiments, each with two
22 technical replicates, were performed, and a representative experiment is shown. (E) Quantification
23 of band intensities from the experiment shown in (D). Bar graphs represent the average and
24 standard deviation (SD) of two biological replicates, each with two technical replicates.
25 Significance was determined by unpaired t-test with Welch's correction. * indicates $p < 0.05$.

26

27 **Figure 2. *In vitro* interaction of DRBD18 with Mex67 and Mtr2.**

28 (A) Recombinant His-tagged Mtr2, GST-tagged DRBD18, and GST were expressed, purified by
29 affinity chromatography, and analyzed by 12.5% SDS-PAGE followed by Coomassie brilliant blue
30 staining. Migration of molecular weight standards (kDa) is indicated on the left. (B) Recombinant
31 GST-DRBD18 or GST were immobilized on glutathione-Sepharose 4B beads, followed by

1 incubation with His-Mtr2 for GST pulldown assays. Western blot analyses were performed using
2 anti-His and anti-GST antibodies to detect His-Mtr2 and GST or GST-DRBD18, respectively.
3 Purified His-Mtr2 (in lane 1), and GST-DRBD18 or GST on glutathione-Sepharose 4B beads
4 incubated without His-Mtr2 were used as inputs for the experiments (in lane 2 and 3 respectively).
5 Two biological replicates, each with two technical replicates, were performed, and a representative
6 experiment is shown.

7

8 **Figure 3. DRBD18 RNAi does not impact tRNA export.**

9 **(A)** *T. brucei* cells harboring the DRBD18 RNAi construct were grown for 23 h in the presence
10 (+Dox) or absence (-Dox) of doxycycline. Total RNA was separated by boronate affinity
11 electrophoresis followed by Northern blotting. A probe recognizing the tRNA^{Tyr} 3' exon was used
12 to detect queuosine (Q)-modified tRNA^{Tyr} levels, based on the electrophoretic shift caused by the
13 presence of Q as described elsewhere (Igloi & Kössel, 1985). G indicates unmodified tRNA^{Tyr}.
14 The levels of Q-modified tRNA are shown below the panel. WT and OX indicate untreated and
15 sodium periodate treated cells as a negative control. A probe against tRNA^{Glu} (middle panel) and
16 the ethidium bromide stained gel (bottom panel) were used as a loading controls. **(B and C)**
17 Subcellular localization of tRNA^{Tyr} (red-Cy3) **(B)** and tRNA^{Glu} (green-AF488) **(C)** in uninduced
18 (-Dox) or induced (+Dox) DRBD18 RNAi cells were monitored by fluorescence *in*
19 *situ* hybridization (FISH). DAPI was used to stain the DNA of the nucleus (N) and the kinetoplast
20 (K). An overlay of the FISH and DAPI signals (Merge) is shown.

21

22 **Figure 4. DRBD18 RNAi causes partial accumulation of mRNA in the nucleus.**

23 PF *T. brucei* cells harboring the DRBD18 RNAi construct were used to assess the relative
24 abundance of mRNA in the nucleus upon depletion of DRBD18. **(A)** Subcellular localization of
25 total mRNA in uninduced (-Dox) or induced (+Dox) DRBD18 RNAi cells was monitored by
26 fluorescence *in situ* hybridization (FISH) using fluorescently labelled oligo(dT). DAPI was used
27 to stain the DNA of the nucleus (N) and the kinetoplast (K). An overlay of the FISH and DAPI
28 signals (Merge) is shown. Bars, 3.2 μ m. Images of individual cells were enlarged to enhance
29 visualization of the nucleus. **(B)** Quantification of the fluorescence intensities of FISH (red-Alexa
30 594) and DAPI (blue) fluorophores were calculated on a line drawn across the nucleus, with
31 overhangs covering the cytosol, using ImageJ (NIH) software. Two biological replicate

1 experiments were performed. The relative intensities represent the average \pm SD from six
2 randomly selected cells (three from each replicate).

3

4 **Figure 5. DRBD18 RNAi inhibits export of a subset of mRNAs from nucleus to cytosol and**
5 **associates with differentially transported mRNAs.**

6 (A) Volcano plot (generated from RNAseq data) of transcripts whose abundance is decreased in
7 cytosol but unchanged in whole cell RNA (corrected p-value <0.05) upon DRBD18 RNAi.
8 Transcripts with fold change (FC) >1.5 are colored blue, and those with FC <1.5 are red.
9 Transcripts analyzed in Fig. 5B are indicated by their TriTrypDB numbers. (B) Representative
10 transcripts, identified by the last four to seven digits of their TriTrypDB numbers, were quantified
11 by qRT-PCR in whole cell and cytosolic fractions. Relative abundance represents RNA levels in
12 induced (+Dox) cells compared to levels in uninduced (-Dox) cells. RNA levels were normalized
13 to 18S rRNA. Values represent the mean of three biological replicates, each with three technical
14 replicates. Significance was determined by unpaired t-test. $**p < 0.01$; $*p < 0.05$. (C) Enrichment
15 of transcripts shown in (B) in anti-DRBD18 immunoprecipitations relative to a non-specific
16 antibody control was measured by UV Cross-Linking ImmunoPrecipitation (CLIP). The 7.7400
17 transcript serves as a negative control. Values represent the mean of three biological replicates,
18 each with three qRT-PCR technical replicates. A value of 1 (dotted line) indicates no enrichment.
19

20 **Figure 6. DRBD18 RNAi causes partial accumulation of export receptors in the nucleus.**

21 (A) The relative abundance of Mtr2 and Mex67 in nuclear and cytosolic fractions in uninduced (-
22 Dox) or induced (+Dox) DRBD18 RNAi cells were analyzed by subcellular fractionation followed
23 by Western blot analysis. Anti-Histone H3 (H3) and anti-EF1 α antibodies were used as loading
24 controls for nuclear and cytosolic fractions, respectively. (B) Quantification of Western blots in
25 (A). Relative abundance of Mex67 or Mtr2 in nuclear and cytosolic fractions was normalized to
26 the expression of Histone H3 and EF1 α , respectively. The normalized protein expression in
27 nuclear and cytosolic fractions from the +Dox were then compared to that of the -Dox (which was
28 set to 1) to calculate the relative abundances in the DRBD18 knockdown. Bar graphs represent the
29 average and standard deviation (SD) of four samples (two biological replicates, each with two
30 technical replicates). Significance was determined by unpaired t-test with Welch's correction. $*p$
31 < 0.05 and ns = non-significant.

1
2
3
4
5
6
7
8
9
10
11
12
13

Figure 7. Model of the role of DRBD18 in mRNA export. A model summarizing the potential role of DRBD18 in mRNA export from nucleus to cytosol through the Nuclear Pore Complex (NPC; see text for details). Inset shows the detailed architecture of NPC and its structural components (Nups). Core scaffold Nups, dark grey (outer ring) and light grey (inner ring); FG Nups, green; nuclear basket, black; cytosolic filament, blue. The NPC has left to right symmetry, and specific features are labeled on only one side for clarity, although they are present on both sides. DRBD18, orange; Mtr2, yellow; Mex67, olive green. DRBD18 may promote association of select mRNAs with Mex67/Mtr2 and likely acts as a chaperone that facilitates passage of the Mex67/Mtr2-DRBD18 mRNP across the NPC due to its interactions with the outer ring and Nup76 complex.

1 **AUTHOR CONTRIBUTIONS**

2

3 A.M., J.K., Z.P. and L.R. designed research; A.M., J.K., A.D., E.H, and M.C. performed research;

4 A.M., J.K., A.D., M.C. and D.M. analyzed data; A.M. and L.R. wrote the paper.

5 **CONFLICT OF INTEREST**

6 The authors declare no conflict of interest.

7

8 **ACKNOWLEDGEMENTS**

9 We are grateful to Kaylen Lott for assistance in the early stages of this work, Mark Carrington
10 for providing anti-Mex67 antibodies, and Brianna Tylec for assistance with figures. This work
11 was supported by National Institutes of Health R01 AI141557 to LKR and Czech Science
12 Foundation [20-11585S to ZP]; ERDF/ESF project Centre for Research of Pathogenicity and
13 Virulence of Parasites [CZ.02.1.01/0.0/0.0/16_019/0000759 to ZP].

14

15

16

17

18

19

20

21

22

23

24

25

26

27

1 REFERENCES

- 2
- 3 Andrews, S., (2010) FastQC: a quality control tool for high throughput sequence data. In.:
4 Babraham Bioinformatics, Babraham Institute, Cambridge, United Kingdom.
- 5 Aphasizheva, I., Alfonzo, J., Carnes, J., Cestari, I., Cruz-Reyes, J., Göringer, H.U., Hajduk, S.,
6 Lukeš, J., Madison-Antenucci, S., Maslov, D.A., McDermott, S.M., Ochsenreiter, T.,
7 Read, L.K., Salavati, R., Schnauffer, A., Schneider, A., Simpson, L., Stuart, K.,
8 Yurchenko, V., Zhou, Z.H., Zíková, A., Zhang, L., Zimmer, S., and Aphasizhev, R.
9 (2020) Lexis and grammar of mitochondrial RNA processing in trypanosomes. *Trends*
10 *Parasitol* **36**: 337-355.
- 11 Aslett, M., Aurrecochea, C., Berriman, M., Brestelli, J., Brunk, B.P., Carrington, M., Depledge,
12 D.P., Fischer, S., Gajria, B., and Gao, X. (2010) TriTrypDB: a functional genomic
13 resource for the Trypanosomatidae. *Nucl Acids Res* **38**: D457-D462.
- 14 Bangs, J.D. (2018) Evolution of antigenic variation in African trypanosomes: Variant surface
15 glycoprotein expression, structure, and function. *Bioessays* **40**: e1800181.
- 16 Braun, I.C., Herold, A., Rode, M., and Izaurralde, E. (2002) Nuclear export of mRNA by
17 TAP/NXF1 requires two nucleoporin-binding sites but not p15. *Mol Cell Biol* **22**: 5405-
18 5418.
- 19 Brugiolo, M., Botti, V., Liu, N., Müller-McNicoll, M., and Neugebauer, K.M. (2017)
20 Fractionation iCLIP detects persistent SR protein binding to conserved, retained introns
21 in chromatin, nucleoplasm and cytoplasm. *Nucl Acids Res* **45**: 10452-10465.
- 22 Büscher, P., Cecchi, G., Jamonneau, V., and Priotto, G. (2017) Human African trypanosomiasis.
23 *Lancet* **390**: 2397-2409.
- 24 Chatterjee, K., Majumder, S., Wan, Y., Shah, V., Wu, J., Huang, H.-Y., and Hopper, A.K. (2017)
25 Sharing the load: Mex67–Mtr2 cofunctions with Los1 in primary tRNA nuclear export.
26 *Genes Devel* **31**: 2186-2198.
- 27 Clayton, C. (2019) Regulation of gene expression in trypanosomatids: living with polycistronic
28 transcription. *Open Biol* **9**: 190072.
- 29 Dean, S., Sunter, J., Wheeler, R.J., Hodkinson, I., Gluenz, E., and Gull, K. (2015) A toolkit
30 enabling efficient, scalable and reproducible gene tagging in trypanosomatids. *Open Biol*
31 **5**: 140197-140197.
- 32 Dobin, A., Davis, C.A., Schlesinger, F., Drenkow, J., Zaleski, C., Jha, S., Batut, P., Chaisson,
33 M., and Gingeras, T.R. (2013) STAR: ultrafast universal RNA-seq aligner.
34 *Bioinformatics* **29**: 15-21.
- 35 Dostalova, A., Käser, S., Cristodero, M., and Schimanski, B. (2013) The nuclear mRNA export
36 receptor Mex67-Mtr2 of *Trypanosoma brucei* contains a unique and essential zinc finger
37 motif. *Mol Microbiol* **88**: 728-739.
- 38 Droll, D., Minia, I., Fadda, A., Singh, A., Stewart, M., Queiroz, R., and Clayton, C. (2013) Post-
39 transcriptional regulation of the trypanosome heat shock response by a zinc finger
40 protein. *PLoS Pathog* **9**: e1003286.
- 41 Ewels, P., Magnusson, M., Lundin, S., and Käller, M. (2016) MultiQC: summarize analysis
42 results for multiple tools and samples in a single report. *Bioinformatics* **32**: 3047-3048.
- 43 Goos, C., Dejung, M., Wehman, A.M., M-Natus, E., Schmidt, J., Sunter, J., Engstler, M., Butter,
44 F., and Kramer, S. (2018) Trypanosomes can initiate nuclear export co-transcriptionally.
45 *Nucl Acids Res* **47**: 266-282.

- 1 Hayman, M.L., Miller, M.M., Chandler, D.M., Goulah, C.C., and Read, L.K. (2001) The
2 trypanosome homolog of human p32 interacts with RBP16 and stimulates its gRNA
3 binding activity. *Nucl Acids Res* **29**: 5216-5225.
- 4 Hegedúsová, E., Kulkarni, S., Burgman, B., Alfonzo, J.D., and Paris, Z. (2019) The general
5 mRNA exporters Mex67 and Mtr2 play distinct roles in nuclear export of tRNAs in
6 *Trypanosoma brucei*. *Nucl Acids Res* **47**: 8620-8631.
- 7 Howard, J.M., and Sanford, J.R. (2015) The RNAissance family: SR proteins as multifaceted
8 regulators of gene expression. *Wiley Interdiscip Rev RNA* **6**: 93-110.
- 9 Igloi, G.L., and Kössel, H. (1985) Affinity electrophoresis for monitoring terminal
10 phosphorylation and the presence of queuosine in RNA. Application of polyacrylamide
11 containing a covalently bound boronic acid. *Nucl Acids Res* **13**: 6881-6898.
- 12 Jensen, R.E., and Englund, P.T. (2012) Network news: the replication of kinetoplast DNA. *Annu*
13 *Rev Microbiol* **66**: 473-491.
- 14 Kafková, L., Debler, E.W., Fisk, J.C., Jain, K., Clarke, S.G., and Read, L.K. (2017) The major
15 protein arginine methyltransferase in *Trypanosoma brucei* functions as an enzyme-p
16 complex. *J Biol Chem* **292**: 2089-2100.
- 17 Keating, J., Yukich, J.O., Sutherland, C.S., Woods, G., and Tediosi, F. (2015) Human African
18 trypanosomiasis prevention, treatment and control costs: A systematic review. *Acta*
19 *Tropica* **150**: 4-13.
- 20 Kessler, A.C., Kulkarni, S.S., Paulines, M.J., Rubio, M.A.T., Limbach, P.A., Paris, Z., and
21 Alfonzo, J.D. (2018) Retrograde nuclear transport from the cytoplasm is required for
22 tRNA(Tyr) maturation in *T. brucei*. *RNA Biol* **15**: 528-536.
- 23 Klebanov-Akopyan, O., Mishra, A., Glousker, G., Tzfati, Y., and Shlomai, J. (2018)
24 *Trypanosoma brucei* UMSBP2 is a single-stranded telomeric DNA binding protein
25 essential for chromosome end protection. *Nucl Acids Res* **46**: 7757-7771.
- 26 Klein, C., Terrao, M., Inchaustegui Gil, D., and Clayton, C. (2015) Polysomes of *Trypanosoma*
27 *brucei*: Association with initiation factors and RNA-binding proteins. *PLoS One* **10**:
28 e0135973.
- 29 Köhler, A., and Hurt, E. (2007) Exporting RNA from the nucleus to the cytoplasm. *Nat Rev Mol*
30 *Cell Biol* **8**: 761-773.
- 31 Kolev, N.G., Ramey-Butler, K., Cross, G.A., Ullu, E., and Tschudi, C. (2012) Developmental
32 progression to infectivity in *Trypanosoma brucei* triggered by an RNA-binding protein.
33 *Science* **338**: 1352-1353.
- 34 Kolev, N.G., Ullu, E., and Tschudi, C. (2014) The emerging role of RNA-binding proteins in the
35 life cycle of *Trypanosoma brucei*. *Cell Microbiol* **16**: 482-489.
- 36 Kopylova, E., Noé, L., and Touzet, H. (2012) SortMeRNA: fast and accurate filtering of
37 ribosomal RNAs in metatranscriptomic data. *Bioinformatics* **28**: 3211-3217.
- 38 Krueger, F. (2015) Trim galore. <https://github.com/FelixKrueger/TrimGalore>
- 39 Li, B., and Dewey, C.N. (2011) RSEM: accurate transcript quantification from RNA-Seq data
40 with or without a reference genome. *BMC Bioinform* **12**: 323.
- 41 Liu, B., Kamanyi Marucha, K., and Clayton, C. (2020) The zinc finger proteins ZC3H20 and
42 ZC3H21 stabilise mRNAs encoding membrane proteins and mitochondrial proteins in
43 insect-form *Trypanosoma brucei*. *Mol Microbiol* **113**: 430-451.
- 44 Lott, K., Mukhopadhyay, S., Li, J., Wang, J., Yao, J., Sun, Y., Qu, J., and Read, L.K. (2015)
45 Arginine methylation of DRBD18 differentially impacts its opposing effects on the
46 trypanosome transcriptome. *Nucl Acids Res* **43**: 5501-5523.

- 1 Love, M.I., Huber, W., and Anders, S. (2014) Moderated estimation of fold change and
2 dispersion for RNA-seq data with DESeq2. *Genome Biol* **15**: 550.
- 3 Martin, M. (2011) Cutadapt removes adapter sequences from high-throughput sequencing reads.
4 *EMBnet. journal* **17**: 10-12.
- 5 Maslon, M.M., Heras, S.R., Bellora, N., Eyras, E., and Cáceres, J.F. (2014) The translational
6 landscape of the splicing factor SRSF1 and its role in mitosis. *Elife* **3**: e02028.
- 7 Matthews, K.R. (2005) The developmental cell biology of *Trypanosoma brucei*. *J Cell Sci* **118**:
8 283-290.
- 9 McAdams, N.M., Simpson, R.M., Chen, R., Sun, Y., and Read, L.K. (2018) MRB7260 is
10 essential for productive protein-RNA interactions within the RNA editing substrate
11 binding complex during trypanosome RNA editing. *RNA* **24**: 540-556.
- 12 Meola, N., and Jensen, T.H. (2017) Targeting the nuclear RNA exosome: Poly(A) binding
13 proteins enter the stage. *RNA Biol* **14**: 820-826.
- 14 Michaeli, S. (2011) Trans-splicing in trypanosomes: machinery and its impact on the parasite
15 transcriptome. *Future Microbiol* **6**: 459-474.
- 16 Mugo, E., and Clayton, C. (2017) Expression of the RNA-binding protein RBP10 promotes the
17 bloodstream-form differentiation state in *Trypanosoma brucei*. *PLoS Pathog* **13**:
18 e1006560.
- 19 Mugo, E., and Erben, E.D. (2020) Identifying trypanosome protein-RNA interactions using RIP-
20 Seq. *Methods Mol Biol* **2116**: 285-294.
- 21 Müller-McNicoll, M., Botti, V., de Jesus Domingues, A.M., Brandl, H., Schwich, O.D., Steiner,
22 M.C., Curk, T., Poser, I., Zarnack, K., and Neugebauer, K.M. (2016) SR proteins are
23 NXF1 adaptors that link alternative RNA processing to mRNA export. *Genes Dev* **30**:
24 553-566.
- 25 Obado, S.O., Brillantes, M., Uryu, K., Zhang, W., Ketaren, N.E., Chait, B.T., Field, M.C., and
26 Rout, M.P. (2016) Interactome mapping reveals the evolutionary history of the nuclear
27 pore complex. *PLOS Biology* **14**: e1002365.
- 28 Rehwinkel, J., Herold, A., Gari, K., Köcher, T., Rode, M., Ciccarelli, F.L., Wilm, M., and
29 Izaurrealde, E. (2004) Genome-wide analysis of mRNAs regulated by the THO complex
30 in *Drosophila melanogaster*. *Nat Struct Mol Biol* **11**: 558-566.
- 31 Rico, E., Ivens, A., Glover, L., Horn, D., and Matthews, K.R. (2017) Genome-wide RNAi
32 selection identifies a regulator of transmission stage-enriched gene families and cell-type
33 differentiation in *Trypanosoma brucei*. *PLoS Pathog* **13**: e1006279.
- 34 Rink, C., and Williams, N. (2019) Unique interactions of the nuclear export receptors TbMex67
35 and TbMtr2 with components of the 5S ribonuclear particle in *Trypanosoma brucei*.
36 *mSphere* **4**: e00471-19.
- 37 Schwede, A., Manful, T., Jha, B.A., Helbig, C., Bercovich, N., Stewart, M., and Clayton, C.
38 (2009) The role of deadenylation in the degradation of unstable mRNAs in trypanosomes.
39 *Nucl Acids Res* **37**: 5511-5528.
- 40 Scott, D.D., Aguilar, L.C., Kramar, M., and Oeffinger, M. (2019) It's not the destination, it's the
41 journey: Heterogeneity in mRNA export mechanisms. *Adv Exp Med Biol* **1203**: 33-81.
- 42 Serpeloni, M., Moraes, C.B., Muniz, J.R., Motta, M.C., Ramos, A.S., Kessler, R.L., Inoue, A.H.,
43 daRocha, W.D., Yamada-Ogatta, S.F., Fragoso, S.P., Goldenberg, S., Freitas-Junior,
44 L.H., and Avila, A.R. (2011a) An essential nuclear protein in trypanosomes is a
45 component of mRNA transcription/export pathway. *PLoS One* **6**: e20730.

- 1 Serpeloni, M., Vidal, N.M., Goldenberg, S., Avila, A.R., and Hoffmann, F.G. (2011b)
2 Comparative genomics of proteins involved in RNA nucleocytoplasmic export. *BMC*
3 *Evol Biol* **11**: 7.
- 4 Strambio-De-Castillia, C., Niepel, M., and Rout, M.P. (2010) The nuclear pore complex:
5 bridging nuclear transport and gene regulation. *Nat Rev Mol Cell Biol* **11**: 490-501.
- 6 Tetenbaum-Novatt, J., and Rout, M.P. (2010) The mechanism of nucleocytoplasmic transport
7 through the nuclear pore complex. *Cold Spring Harb Symp Quant Biol* **75**: 567-584.
- 8 Tudek, A., Schmid, M., and Jensen, T.H. (2019) Escaping nuclear decay: the significance of
9 mRNA export for gene expression. *Curr Genet* **65**: 473-476.
- 10 Tudek, A., Schmid, M., Makaras, M., Barrass, J.D., Beggs, J.D., and Jensen, T.H. (2018) A
11 nuclear export block triggers the decay of newly synthesized polyadenylated RNA. *Cell*
12 *Rep* **24**: 2457-2467.e2457.
- 13 Tutucci, E., and Stutz, F. (2011) Keeping mRNPs in check during assembly and nuclear export.
14 *Nature Rev Mol Cell Biol* **12**: 377-384.
- 15 Verner, Z., Basu, S., Benz, C., Dixit, S., Dobáková, E., Faktorová, D., Hashimi, H., Horáková,
16 E., Huang, Z., Paris, Z., Peña-Díaz, P., Ridlon, L., Týč, J., Wildridge, D., Zíková, A., and
17 Lukeš, J. (2015) Malleable mitochondrion of *Trypanosoma brucei*. *Int Rev Cell Mol Biol*
18 **315**: 73-151.
- 19 Wickramasinghe, V.O., Andrews, R., Ellis, P., Langford, C., Gurdon, J.B., Stewart, M.,
20 Venkitaraman, A.R., and Laskey, R.A. (2014) Selective nuclear export of specific classes
21 of mRNA from mammalian nuclei is promoted by GANP. *Nucl Acids Res* **42**: 5059-5071.
- 22 Wickramasinghe, V.O., and Laskey, R.A. (2015) Control of mammalian gene expression by
23 selective mRNA export. *Nat Rev Mol Cell Biol* **16**: 431-442.
- 24 Zimmer, S.L., Simpson, R.M., and Read, L.K. (2018) High throughput sequencing revolution
25 reveals conserved fundamentals of U-indel editing. *Wiley Interdiscip Rev RNA*: e1487.
26
27

Figure 1

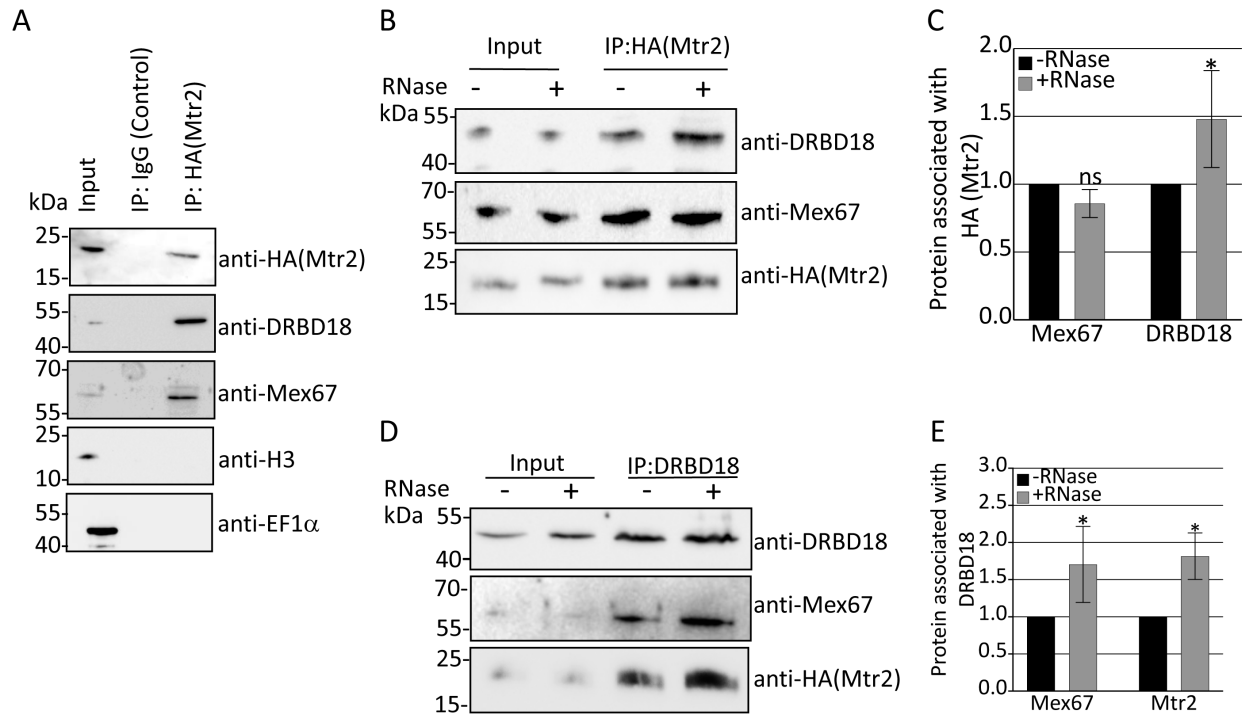
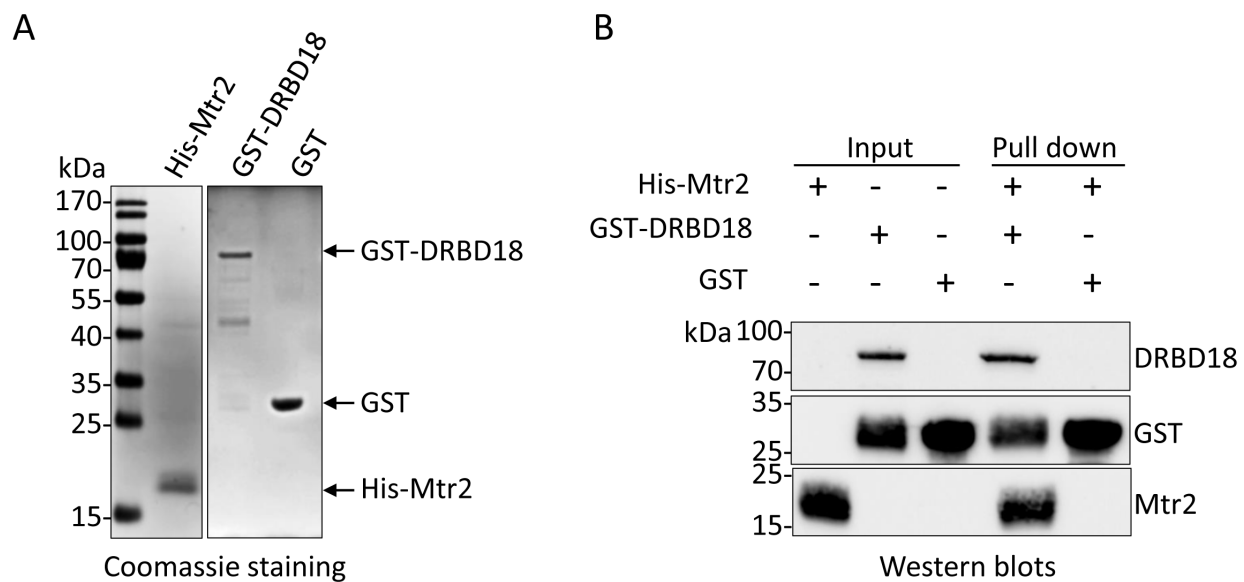


Figure 2



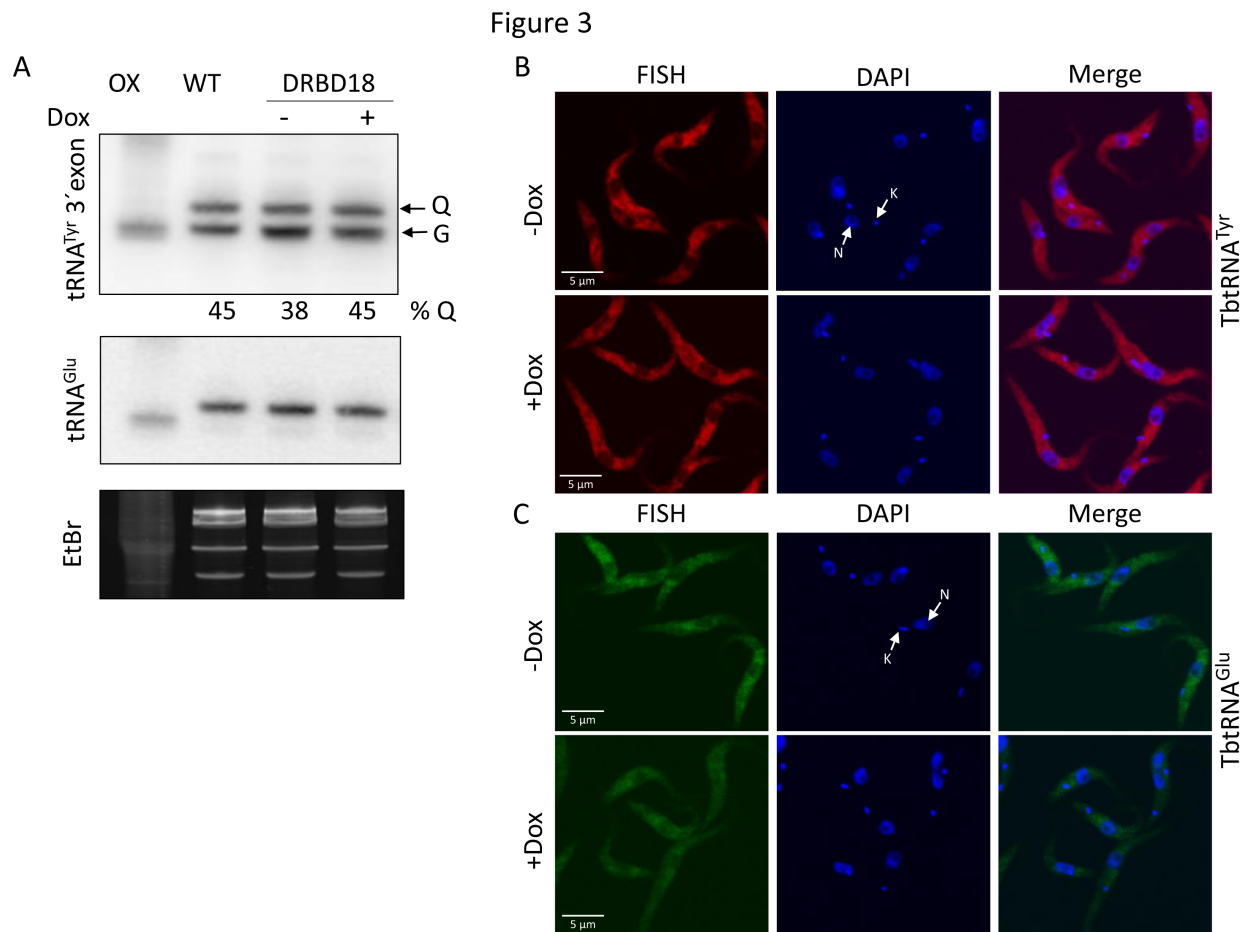


Figure 4

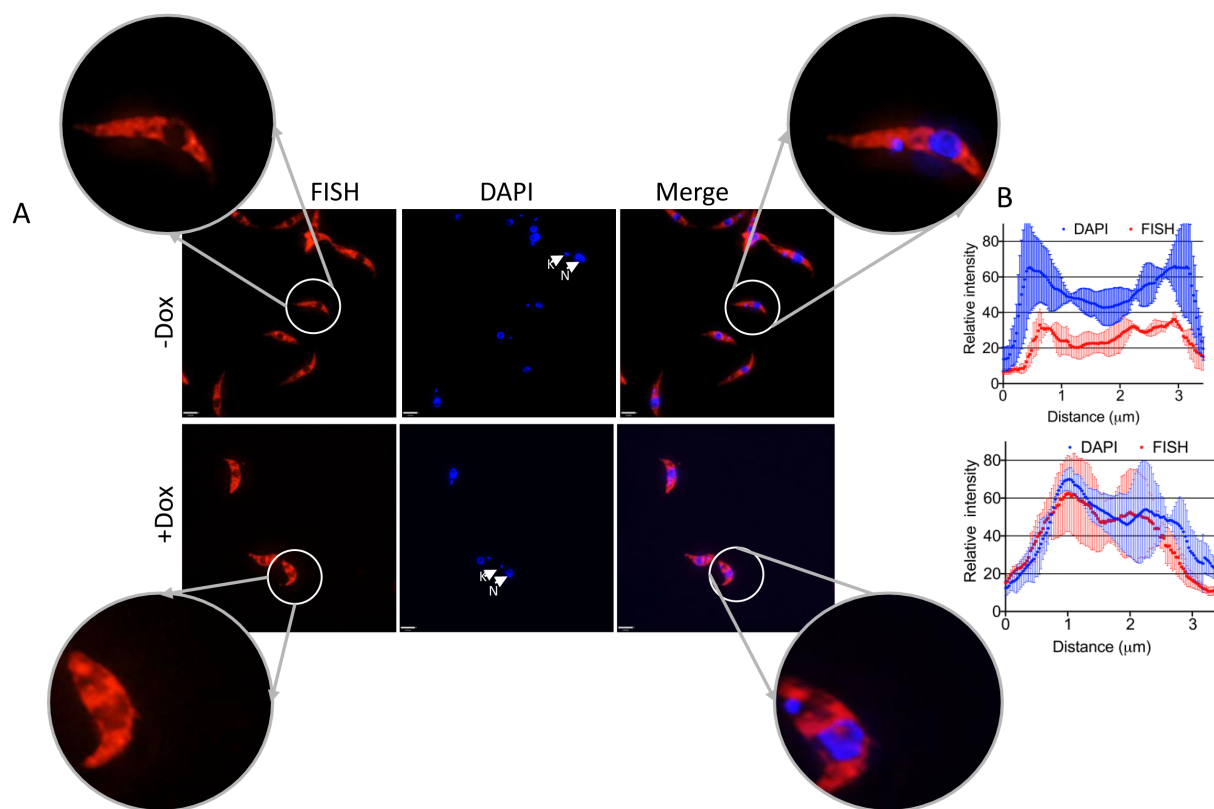


Figure 5

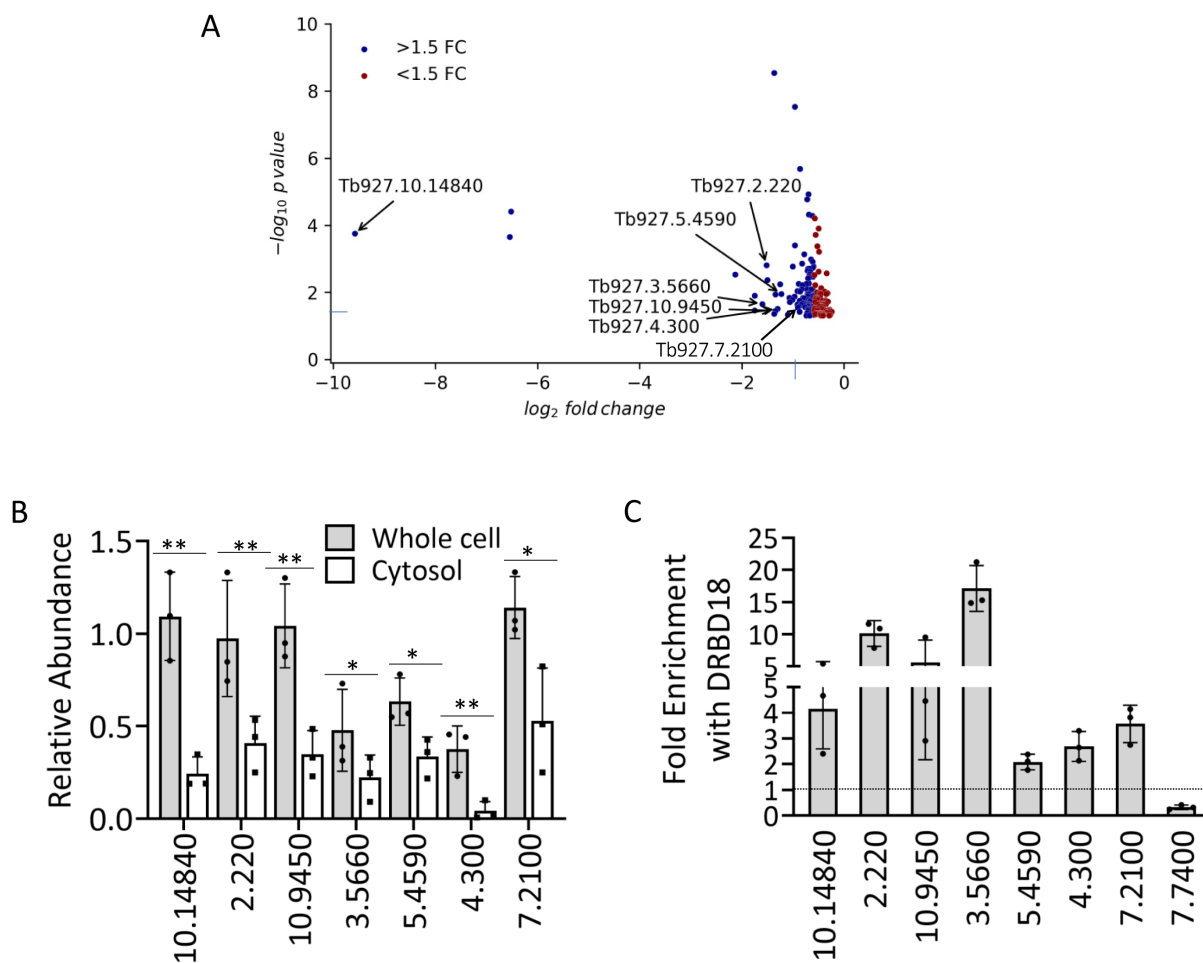
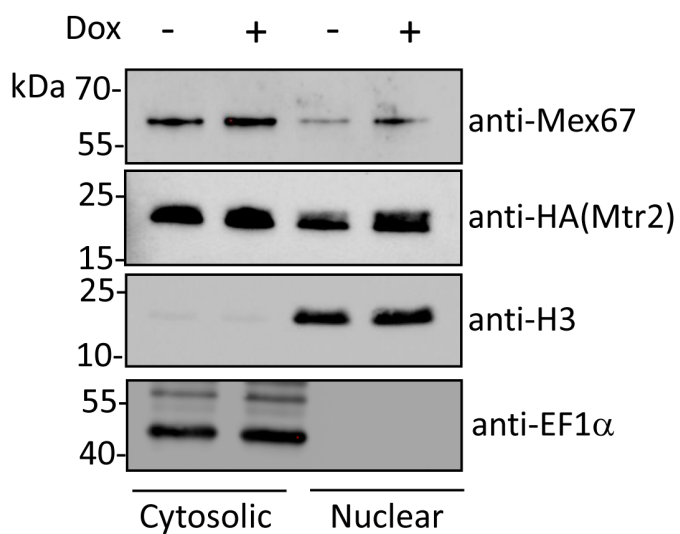


Figure 6

A



B

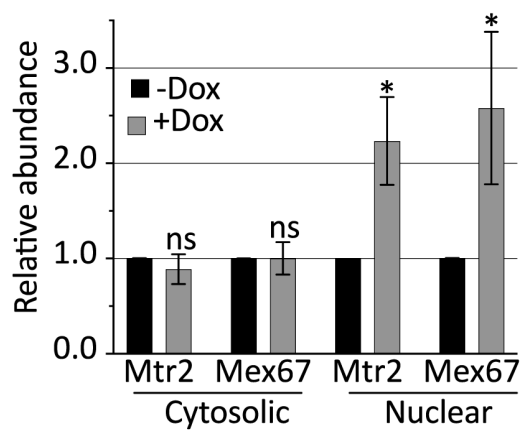


Figure 7

